Nuclear Inst. and Methods in Physics Research, A 971 (2020) 164112

Contents lists available at ScienceDirect

Nuclear Inst. and Methods in Physics Research, A

journal homepage: www.elsevier.com/locate/nima

A survey of space radiation damage to DAMPE-PSD

Yongjie Zhang [a,b,d,e], Zhiyu Sun [a,e], Yuhong Yu [a,e,*], Jianhua Guo [c,f], Fang Fang [a], Yong Zhou [a], Zhaoming Wang [a], Yapeng Zhang [a,e], Bitao Hu [d]

[a] Institute of Modern Physics, Chinese Academy of Sciences, 509 Nanchang Road, Lanzhou, 730000, PR China
[b] Graduate University of the Chinese Academy of Sciences, 19A Yuquan Road, Beijing, 100049, PR China
[c] Key Laboratory of Dark Matter and Space Astronomy, Purple Mountain Observatory, Chinese Academy of Sciences, Nanjing 210008, PR China
[d] School of Nuclear Science and Technology, Lanzhou University, 222 South Tianshui Road, Lanzhou, 730000, PR China
[e] School of Nuclear Science and Technology, University of Chinese Academy of Science, Beijing 100049, PR China
[f] School of Astronomy and Space Science,University of Science and Technology of China, Hefei 230026, PR China

ARTICLE INFO

Keywords:
DAMPE
PSD
PMT
Working lifetime
SAA region

ABSTRACT

As a new astronomical telescope for cosmic rays, DArk Matter Particles Explorer (DAMPE) have been operated in-orbit for more than four years since it was launched at the end of 2015. It could measure electron and gamma-ray ranging from 5 GeV to 10 TeV to explore the brand new astrophysical phenomenon. As a very high energy telescope, the working lifetime is significant to accumulate high statistics for astroparticle signals. The aging of detectors due to the Total Absorbed Dose (TAD) is one of the main factors affecting the working lifetime of DAMPE. Due to the Plastic Scintillator Detector (PSD) should face a worse radiation environment, in this paper, the space TAD damage to the scintillator strips and the PhotoMultiplier Tubes (PMTs) of the PSD are investigated in detail. The results show that the radiation damage to the PSD strips can be ignored during DAMPE satellite operation time, and the minimum working lifetime of the PMTs in the PSD is 8.32 years as the gain of the PMTs are degraded by 20% in orbit.

1. Introduction

In China, an astrophysics observatory named DArk Matter Particle Explorer (DAMPE) has been launched into a sun-synchronous orbit at the end of 2015. Its primary aim is to measure the spectra features of stable products from dark matter decay or annihilation, such as electrons and gamma-rays in a broad energy range covering from 5 GeV to 10 TeV with a very excellent resolution (1.5% at 800 GeV) [1–3]. Meanwhile, it is also used to identify nuclei species up to Fe ($Z = 26$) to study the flux spectrums of primary and secondary cosmic rays for understanding the acceleration in the celestial sources and the propagation in the Galaxy [4–6].

As a very high energy telescope, it is challenging to accumulate high statistics for astroparticle signals since cosmic rays obey the exponential decay law approximately [5]. This always requires an apparatus has a sizeable geometrical acceptance as well as a long operation time. An apparatus with a large area and solid angle can receive more cosmic rays in a unit time. This factor has been decided at design time. The acceptance is mainly dependent on the structure of the apparatus, and it cannot be changed in-orbit operation. The working lifetime of an apparatus can also extend the statistics of cosmic rays since the whole recording time would be increased, and the minimum expected lifetime of DAMPE is 3 years from statistical evaluation to obtain adequate good events.

In general, due to the existence of a natural space radiation environment, it is very different for the same apparatus operating on the ground and in orbit since the accumulation of radiation dose could accelerate the aging of materials and electronic components. It is well known that ionizing radiation in outer space mainly consists of three types of sources: protons and electrons trapped by the Earth's Van Allen radiation belt, Solar Energetic Particles (SEPs) and galactic cosmic rays. As a low earth orbit sun-synchronous satellite, the daily dose rate of DAMPE is not too serious because of the geomagnetic cutoff for low energy cosmic rays. Unfortunately, a special region known as the South Atlantic Anomaly (SAA) behaves an anomaly in the inner radiation belts, and the trapped proton and trapped electron fluxes in this region are many orders of magnitude higher than the fluxes seen over most of the orbit. According to AP8 and AE8 models [7], the maximum energy of trapped protons and trapped electrons will not exceed 400 MeV and 7 MeV, respectively. DAMPE will pass through the SAA region typically ten times a day, with each passage lasting a few to ten minutes, and it would result in the accumulation of large TAD since the mission durations of DAMPE would last for a long time. Besides, the particle fluxes will increase in the High Latitude Regions

* Corresponding author at: Institute of Modern Physics, Chinese Academy of Sciences, 509 Nanchang Road, Lanzhou, 730000, PR China.
E-mail address: yuyuhong@impcas.ac.cn (Y. Yu).

https://doi.org/10.1016/j.nima.2020.164112
Received 20 December 2019; Received in revised form 5 May 2020; Accepted 5 May 2020
Available online 7 May 2020

(HLRs) as SEPs explode. This cumulative absorbed dose will cause the performance of DAMPE gradually deteriorating, and make the observed scientific data invalid and even key component damage. Thus it is vital to investigate the radiation dose level of DAMPE and to take some protective countermeasures in the design time.

As Fig. 1 shown, DAMPE consists of four sub-detectors, (1) a Plastics Scintillator Detector (PSD), mainly used in electrons/photons discrimination and charge measurement, (2) a Silicon Tungsten Tracker (STK), providing track information as well as charge measurement, (3) a BGO electromagnetic calorimeter (BGO), designed to measure the energy of incident particles and reject proton background, and (4) a neutron detector (NUD), assisting BGO to reject proton background. More details about sub-detectors can refer to descriptions [8–12]. Due to the top location outside of DAMPE satellite, PSD will face a worse radiation environment. Thus it is meaningful to evaluate radiation damage by taking the PSD as an example.

2. The PSD description

As shown in Fig. 2(a), the PSD with an effective active area of 825 mm × 825 mm is designed to adopt a segmented configuration with two layers being perpendicular to each other. Each layer has 41 scintillator strips made of EJ-200 [13] with a dimension of 884 mm × 28 mm (25 mm for the strips around the edges)×10 mm and adjacent strips in each layer are overlapped by 8 mm as shown in Fig. 2(b). Each strip is numbered from left to right in sequences. The even strips is located at a higher position than the odd strips in top layer and a lower position in bottom layer. The scintillation light converted from energy deposition will be read out by two Photomultiplier Tubes (PMTs) coupled to each end of the strip. The signals from each PMT are feed into Front End Electronics (FEE) Modules. After sampling, holding and processing, the analog signals are converted to digital data and transmitted to the data management system of satellite.

In order to avoid the damage from the harsh environments during the launch, a Carbon Fiber Reinforced Plastics (CFRP) material with a density of 1.62 g/cm^3 is used as the main support structure for PSD. For reducing the total weight of the PSD furtherly, the bottom plate adopts a sandwich structure of an aluminum honeycomb plane (a mean effective density of 0.068 g/cm^3) with two CRFP skins on both sides. Meanwhile, to balance the rigidity and the weight of the bottom plate, some CFRP cubic hollow tubes are stuck on the inner surface of the bottom plate to fix the scintillator strips. This design is also used to the bottom cover plate and top cover plate, and there are 82 scintillator strips in total fixed by these CRFP cubic hollow tubes. Compared with the scintillator strips, the readout PMTs are a kind of vacuum glass device, and their mechanical properties are very fragile. To solve this problem, the PMTs are potted with two different types of RTV silicones [14] RTV118 and RTV615, and then placed in hollow holes on an aluminum crossbeam as shown in Fig. 2(c). Besides, a top plate installed above the top cover plate for light shielding and for stopping low energy particles also adopts a sandwich structure like the bottom plate, while there are no CFRP cubic hollow tubes stuck on.

As a vital part of DAMPE, the PSD performance will degrade or be damaged in the space radiation environment, which is a critical issue throughout the design and construction of the PSD. So it is important to understand the mechanisms that might cause degradation or damage. Meanwhile, it is necessary to make radiation tests and radiation hardening design for electronic ASIC components or detection material to assure that they will withstand the harsh environments in space. According to the classification of time scale, there are two types of damage caused by the radiation environment to spacecraft that can be distinguished. One of these classes is a transient effect, namely Single Event Effect (SEE), where a single particle causes a piece of equipment to malfunction. This effect is mainly observed from microelectronic devices, such as the ASIC component. The other is long term effect, namely Total Absorbed Dose (TAD), which is contributed by ionizing energy loss related to Total Ionizing Dose (TID) and non-ionizing energy loss related to Displacement Damage Effect (DDE). As a LEO space satellite, TAD is mainly contributed by the SAA region and the HLRs, especially in the SAA region for the high particle fluxes in this region, are many orders of magnitude higher than the fluxes seen over most the orbit. As a conventional space radiation detector in low orbit, this type of radiation damage is sensitive to the entire PSD system. For convenience, the PSD could be classified to be three main parts: mechanical supports, electronic parts and detection parts. The mechanical supports used in the PSD are not sensitive to various types of radiation damage, and the radiation effects of SEE and TAD should be considered in the design of electronic parts carefully. The detection parts in the PSD mainly include two parts: the plastic scintillator strips and the PMTs. Since these two parts are not sensitive to SEE, the radiation effect on them is dominated by TAD. Generally, TID is the main factor leading to the aging of PSD scintillator strip and PMT degradation, and the contribution from DDE is a tiny proportion in TAD. In contrast to electronics, few reports are focusing on the radiation effect of the plastic scintillator detectors readout by PMTs in orbit, especially for the working lifetime of the PMTs in orbit.

In this paper, the space total absorbed dose damage to the scintillator strips, and TAD damage to the PMTs of the PSD in the orbit are reported. A working lifetime protection design to the PMTs to avoid excessive exposure in the given sun-synchronous orbit and verification tests for the protection design is also reported.

Table 1
Orbit parameters of DAMPE.

Orbit parameters	Value
Apogee	505 Km
Perigee	484 Km
Inclination	97.3019°
Right ascension of the ascending node	66.8175°
Argument of perigee	99.6566°
Mean anomaly	329.4928°

3. Evaluation of space radiation effects

3.1. Main space radiation sources of DAMPE

During their missions spent in space, many space apparatuses like DAMPE are exposed to radiation particles with various charges and energies. The focus on this paper is the subject of the space radiation damage to the detection parts of the PSD, so it needs to evaluate the TAD of the space environment radiation in a given orbit of DAMPE. A web-based software named Space Environment Information System (SPENVIS) [15] has been chosen to survey the outside space radiation environment for DAMPE. When using Spenvis software packages, the orbit parameters of DAMPE must be defined firstly by the user. The initial orbit parameters of sun-synchronous orbit for DAMPE are listed in Table 1. The low earth orbit determines that DAMPE will run inside the earth's magnetosphere. Due to the existence of the earth magnetic field, a large number of energetic charged particles are captured by the Lorentz force of the field, which forms the so-called Van Allen radiation belt. In SPENVIS, there are different models for energetic charged particles. As for the trapped protons in this radiation belt, the models including AP8, CRRESPRO and SAMPEX/PET PSB97 can be selected. As for the trapped electrons in this radiation belt, there are other models such as AE8, CRRESELE and the AE8MIN ESA-SEEI can be available. The models AP8 and AE8 are chosen in our survey. As for the galactic cosmic rays, it is evaluated based on the old CREME version of Spenvis. Fig. 3 shows the differential fluxes of different sources given by Spenvis, where the average proton energy spectrum ranging from 0.1 MeV to 400 MeV and the electron spectrum with energies ranging from 0.04 MeV to 7 MeV for a long term mission are provided by the solar maximum and the minimum conditions according to the AP8 and

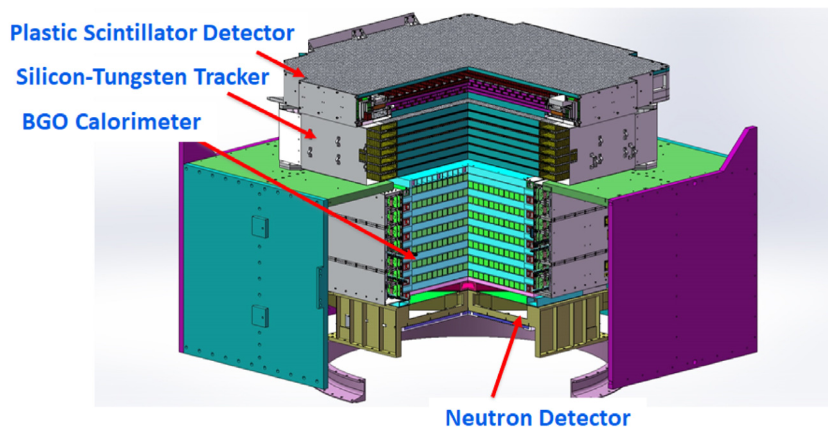

Fig. 1. Schematic diagram of DAMPE.

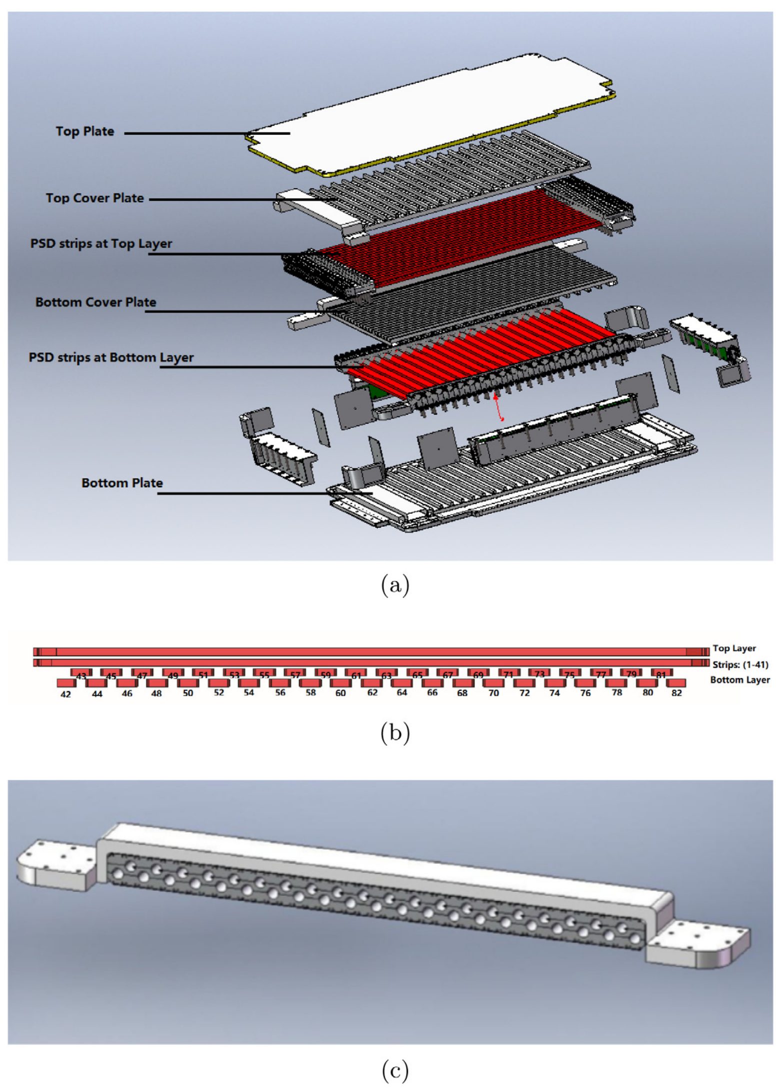

Fig. 2. (a) The exploded view of the PSD. (b) The side view of the PSD strips. (c) The aluminum crossbeam used to fix the PMTs.

AE8 models. As shown in the figure, the trapped protons fluxes near the solar maximum are smaller compared with the solar minimum one. The reason is that the solar ultraviolet (UV) input causes the atmosphere to expand at solar maximum, and the increased atmosphere height causes the trapped particles to be removed from the radiation belts. However, for DAMPE, due to its running sun-synchronous orbit, the trapped electrons cannot be ignored since it will pass through HLRs per orbit, where the trapped electron flux is higher than other regions because of SEP explosion. In order to evaluate the maximum radiation damage, the trapped particle fluxes obtained by AP8MIN and AE8MAX are adopted in the following. Besides, due to the radiation from galactic cosmic rays is fairly less than the trapped protons and electrons, the

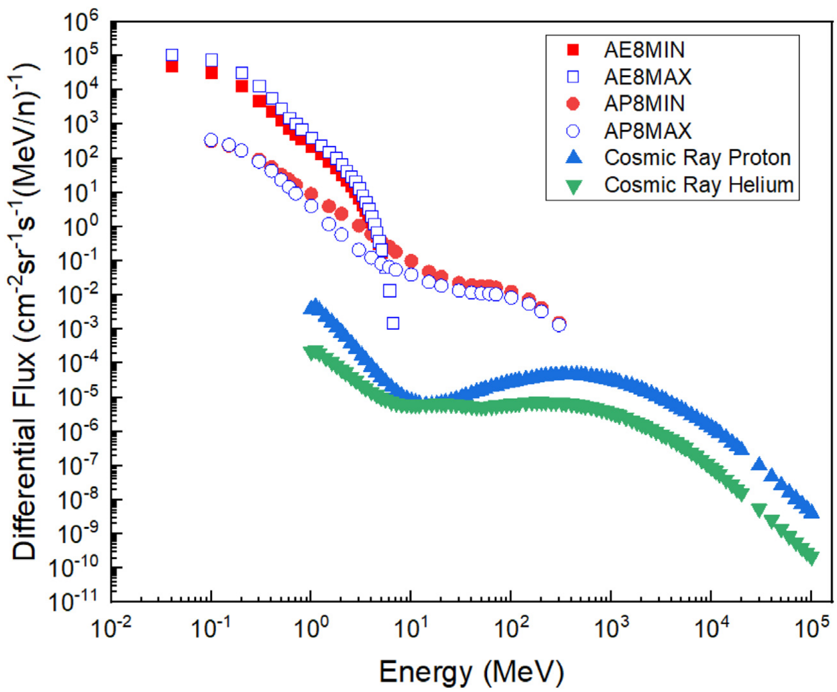

Fig. 3. The spectra of radiation charged particles at the orbit of DAMPE. Red solid square stands for AE8 model for electron at solar minimum condition, blue hollow square stands for AE8 model at solar maximum condition, red solid circle stands for AP8 model for proton at solar minimum condition, blue hollow circle stands for AP8 model at solar maximum condition, blue triangle represents cosmic ray proton and green inverted triangle represents cosmic ray helium. (For interpretation of the references to color in this figure legend, the reader is referred to the web version of this article.)

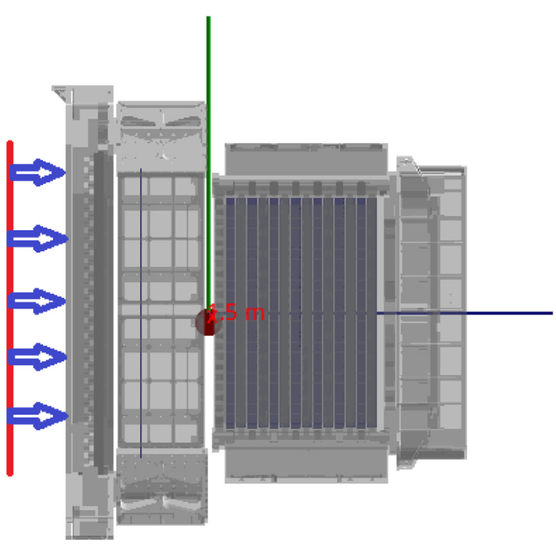

Fig. 4. The DAMPE geometric configuration formed by a GDML.

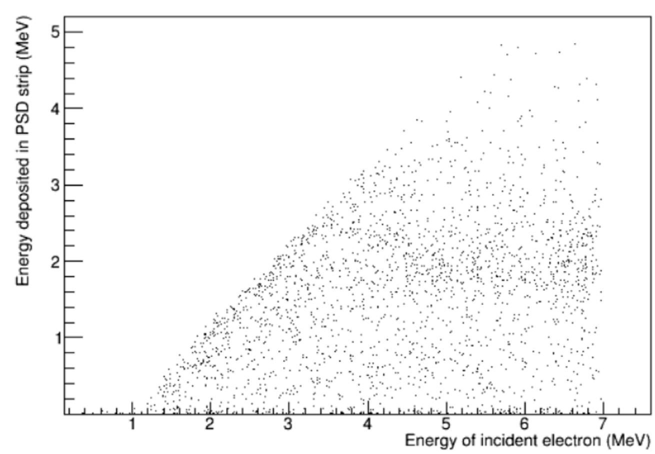

Fig. 5. Energy deposition versus energy of incident electrons.

contribution from galaxy cosmic rays can be ignored. In a word, the trapped protons and electrons in Van Allen radiation belt are the main source contributing to space radiation for DAMPE.

3.2. Radiation effect of shielding material

As mentioned in previous sections, the PSD at DAMPE satellite will face a worse particle radiation environment, and a thick shielding material is remarkably enough to reduce the radiation damage. However, to reduce the reaction probability with incident particles, the minimum thickness of non-sensitive detection above the scintillator strips of the PSD is required by DAMPE, mostly contributed by the top plate and the top cover plate as shown in 2(a). By contrast, a skinny thickness used to the top plate will result in the rigidity decrease of the top plate. At the final design, a 3 mm CRFP thick top plate with a sandwich structure is selected for its light nuclear charge number and high mechanical rigidity. Lots of low energy particles have no chance to hit the scintillator strips and will be stopped in this plate, so these low energy particles have no contribution to TAD of the detection parts. Thus the minimum energy required for a proton or electron to penetrate the plate should be calculated based on the Geant4 simulation.

In order to evaluate the TAD of the sensitive detection parts accurately, it is important to obtain the threshold energy value of the incident particles which can enter into the sensitive detection parts. According to the previous analysis results from SPENVIS software, the incident particles dominate by trapped electrons and trapped protons, so the question turns to obtain the cut-down energy values of trapped electrons and protons. An offline analysis package toolkit named DAMPE software (DMPSW) [16] has been developed by DAMPE

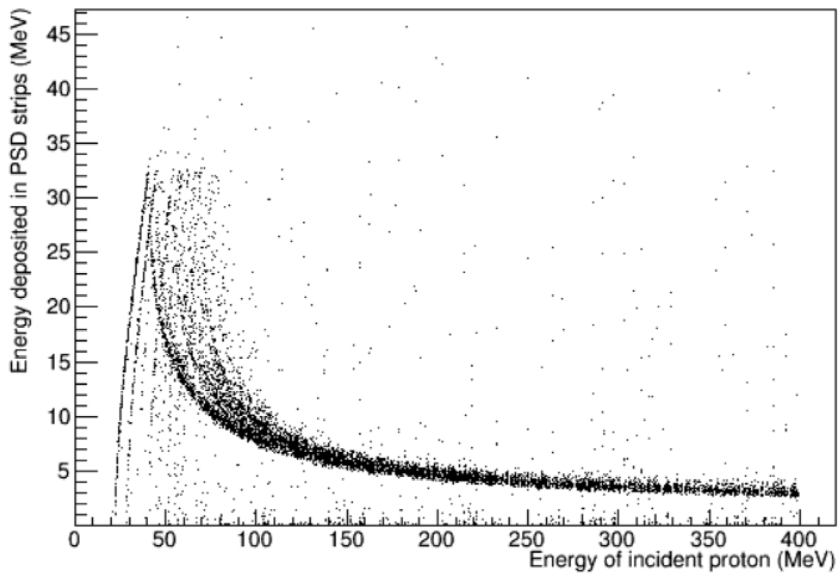

Fig. 6. Energy deposition versus energy of incident protons.

collaboration, where a simulation module based on Geant4 [17] has been developed to describe the geometry structure and material information and simulate the behaviors of incident particles in the detector. The concrete geometry parameters of DAMPE are defined by a Geometry Description Markup Language (GDML) [17] in detail, and the final configuration of the effective payload of DAMPE is shown in Fig. 4. In this figure, a square plane particle source is set in front of DAMPE in minus z-direction, and the direction of incident particles is set to be perpendicular to the x-y plane for the shortest path length as passing through. The primary input energy range of electrons covers from 500 KeV to 7 MeV and protons from 1 MeV to 400 MeV. Figs. 6 and 5 are scattering plots of energy depositions in the PSD strips vs. incident primary energy of the trapped electrons and protons, respectively. It demonstrates that only the electrons above 1 MeV and the protons above 20 MeV can penetrate the non-sensitive materials and deposit energy in the scintillator strips.

4. Evaluation of radiation damage to the PSD strips

4.1. Hit rates to the PSD strips

Since the existence of the top plate and the top cover plate, only particles above an energy threshold have a contribution to the TAD of the PSD strips, so only the trapped particles exceeding its energy thresholds are taken into consideration. After inputting orbit parameters of DAMPE in SPENVIS, Figs. 7 and 8 show the distribution maps of the trapped proton (>20 MeV) and the trapped electron (>1 MeV) at 500 Km altitude, respectively. From both figures, the two trapped particles in the SAA region are distinct. The trapped protons are negligible outside the SAA region, while the flux of trapped electrons can also be very high in HLRs, which are mainly contributed by the burst of SEPs. From an evaluation, the expected operation time of DAMPE stays in the SAA region is about 5% of the whole running time for the trapped protons. For the trapped electrons, this ratio increases to $\frac{1}{3}$ for the extra influence from HLRs, as shown in Fig. 7. Thus it is reasonably considered that the flux of the trapped protons covering the energy range from 20 MeV to 400 MeV in the SAA region is about 20 times the average flux value of the whole orbit as shown in Fig. 3. Likewise, the flux of the trapped electrons with an energy range from 1 MeV to 7 MeV is about 3 times the average flux in the same energy range when DAMPE runs in HLRs and SAA.

For evaluating the hit rates on each PSD scintillator strip in detail, a 4π sphere source with 1.38 m radius is set around DAMPE in DMPSW code, and the emitting direction of particles obeys cosine law. In order to obtain the maximum hit rates of the space radiation environment at a given orbit, the energy spectrum of the trapped proton samples of the sphere sources adopts the flux in minimum solar conditions based on AP8 model, and the energy spectrum of the trapped electrons employs the flux in maximum solar conditions according to AE8 model (the energy spectrum as shown in Fig. 3). Since the contributions to the trapped protons are only concentrated in the SAA region and the flux of the trapped protons is an average value in SPENVIS, to evaluate the hit rates in the extreme radiation conditions, the maximum hit rates on each PSD strip should multiply by the factor of 20. For the trapped electrons, this factor value is 3.

The simulation results are shown in Figs. 9(a) and 9(b). These figures give the distribution of the maximum hit rates of each PSD strip for the trapped protons and electrons respectively, where PSD strips number 1–41 represents strips installed at top layer and the number 42–82 installed at bottom layer. It is obviously found that the maximum hit rates of the strips at the top layer are higher than the strips at the bottom layer. Additionally, it is also obviously found that the maximum hit rates of the even strips are higher than the odd strips at the top layer because of the overlapping structure design used for the adjacent strips at the same layer. So the even strips at the top layer should face the harshest space radiation environments, and the maximum hit rates of the PSD strips for the trapped protons and electrons will not exceed 240 KHz and 300 KHz respectively.

4.2. TAD for the PSD strips

The TAD is defined as the energy deposition in detection material through ionizing or non-ionizing radiation process by unit mass, which can be described by formula (1) and used to evaluate the absorbed dose radiation damage to the PSD strips.

$$TAD = \int \frac{dE}{dm}(t)dt \qquad (1)$$

In formula (1), dE represents energy deposition for the trapped particles hitting, and dm stands for the mass of each PSD strip. The density of scintillator material is 1.023 g/cm^3, and the mass of each scintillator strip with an effective volume of 884 mm$\times$28 mm (25 mm for the strips at the edges)$\times$10 mm is about 0.236 kg(0.211 Kg). Fig. 10 illustrates the TAD simulation results of each PSD strip. In this figure, it is found that the TAD contribution from the trapped protons is higher than the trapped electrons, although the hit rates of the trapped protons are less

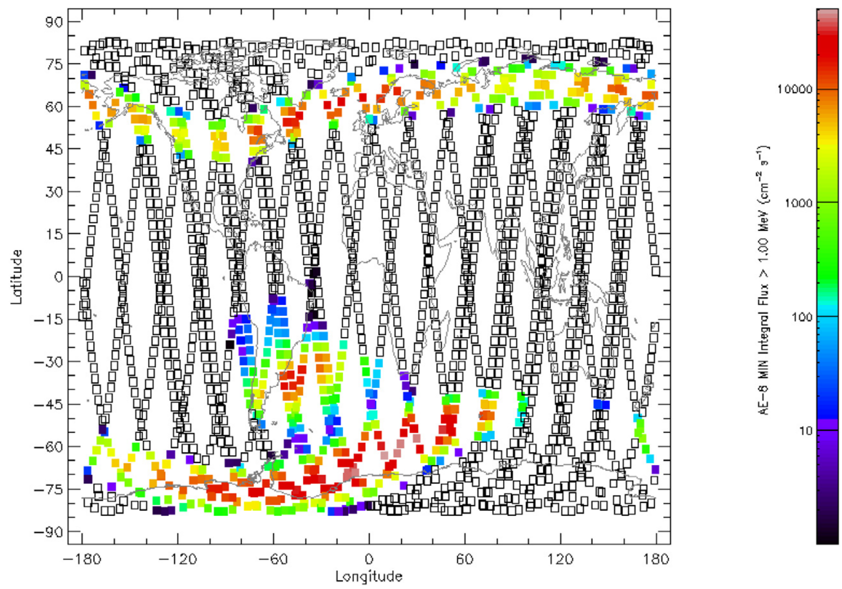

Fig. 7. The distribution of orbital electron flux from a Spenvis calculation (>1 MeV).

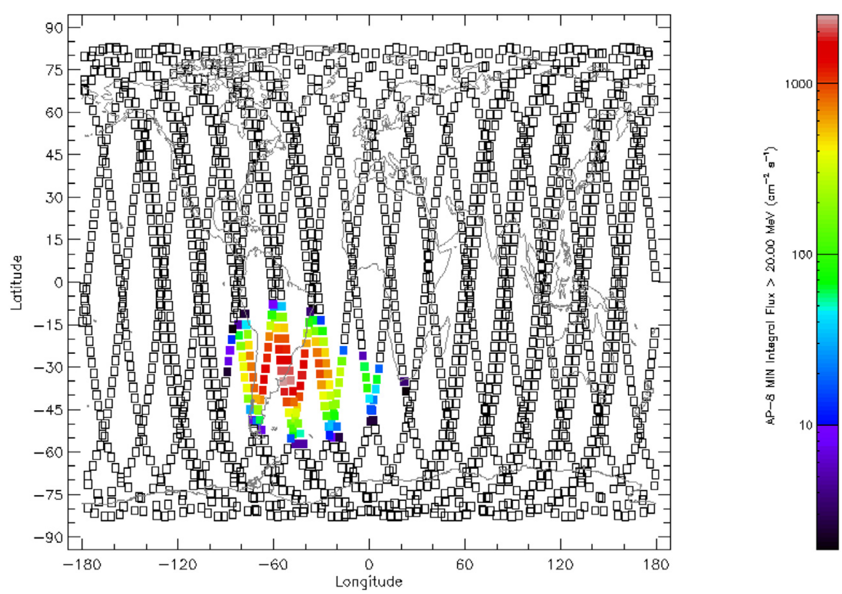

Fig. 8. The distribution of orbital proton flux from a Spenvis calculation (>20 MeV).

than the trapped electrons. The reason is that the energy deposition behavior of electrons is very different from protons. As shown in Fig. 6, the energy deposition will increase to a maximum then decrease according to Beth–Bloch laws, and the maximum value is about 40 MeV. This value is one order of magnitude larger than the maximum energy loss of the trapped electrons, as shown in Fig. 5. Additionally, for all the PSD strips, the same odd–even effect as hit rates can be found, and the strips installed at top layer suffer the maximum radiation dose within 4 Gy per year. According to some previous researches for radiation hardness of EJ-200 scintillator [18,19], the performance of EJ-200 such as emission, transmission spectrum and light yield has no significant change even if it accepts radiation dose 600 Gy. The PSD scintillator strips in the space environment accept 4 Gy per year, which is far less than the safe dose. Thus the space radiation damage to the PSD strips can be ignored during DAMPE satellite operation time.

5. Evaluation of radiation damage to the PMTs

Since invented about 80 years ago, PMTs have been widely used in nuclear and particle experiments due to the high sensitivity, large gain, fast time response and other advantages. The use of many PMTs in satellite-borne scientific research experiments dramatically expands the scope of the application of the photodevice. When these tubes are used in space research applications, they should be adopted a ruggedized version that can resist vibration and shock since they are operated in a harsh mechanics environment. Of course, they should be able to detect low light levels in general. Beyond these, another concern is the working lifetime of the tubes, since they are subjected to TAD from various ionizing particles in orbit. Different from the scintillator strip, exposure to abundant high energy particles directly will make the performance of the PMT window transparency gradually degrade, which leads to the dark current increasing considerably and the PMT gain degradation gradually. In extreme cases, excessive exposure to

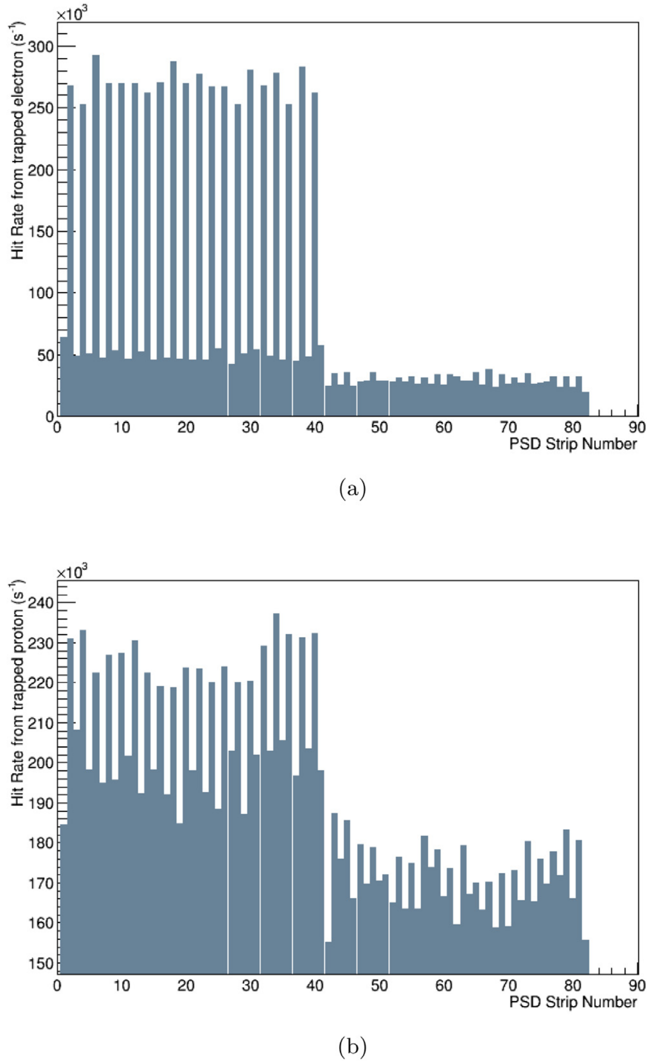

Fig. 9. (a) The distribution of hit rates on the PSD different strips for the trapped electrons. (b) The distribution of hit rates on the PSD different strips for the trapped protons.

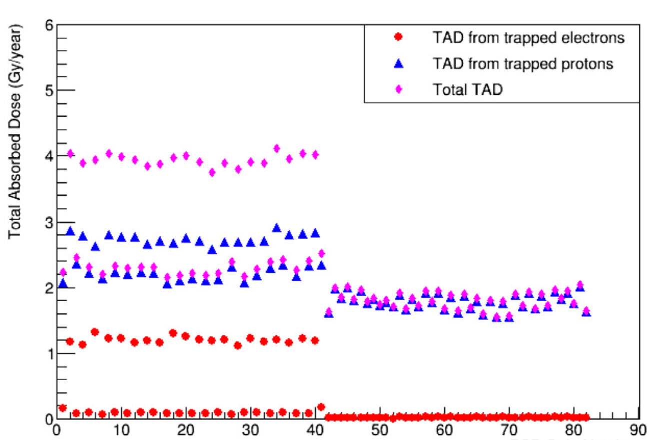

Fig. 10. The distribution of TAD of each PSD strip for the trapped particles. The red circles represent TAD related to the trapped electrons, and the blue triangles stand for TAD related to the trapped protons. The purple diamond is the TAD. (For interpretation of the references to color in this figure legend, the reader is referred to the web version of this article.)

radiation particles or large current produced by massive scintillation lights even cause the device broken.

5.1. Design of PMT voltage divider

The PMTs used in the PSD are manufactured by Hamamatsu Photonics and their type is $R4443$. This is a head-on PMT with 10-stage, a minimum effective area of $\phi 10$ mm, quantum efficiency is about 18% at 375 nm, and a typical gain of 10^6. By measuring the energy depositions of particles from electrons, protons and heavy ions up to Z = 26, a large dynamic range covering from 0.1 MIPs to 1400 MIPs is required. In order to solve this problem, a circuit of double-dynode readout is used to design the PMT voltage divider of the PSD, as shown in Fig. 11. Two dynodes, one is dynode 5 (Dy5), and the other is dynode 8 (Dy8), are used to extract the PMT signal. The Dy5 is used to deal with the larger signal for its small gain, while the Dy8 is used to deal with the smaller signal for its large gain. High count rates in the SAA region can cause a possible large immediate current, which brings damage to the PMT ant the high voltage power supply. In order to protect the PMT and the high voltage power supply, a total resistance value of the PMT voltage divider is set to be 61.2 Mohms, and the maximum current that can flow is less than 13 uA. This current is far higher than the tube needs in normal operation, but low enough that the tube would not suffer immediate damage. The PMT voltage divider circuit of the PSD is shown in Fig. 11, and a detailed description of this divider design can refer to the paper [20]. Besides, this PMT is a ruggedized version to reduce the risk of damage from shocks and vibrations in the launch phase. In order to fix the PMTs, an aluminum crossbeam with many holes has been designed, as shown in Fig. 2(c). The crossbeam also can reduce the probability of radiation particles hitting the PMTs directly. Taking into account the 3 mm thick top plate and other mechanical supports, the PMTs are under proper radiation particle shielding. The same method as shown in Fig. 4 was adopted to simulate the shielding effect of PMT. The simulation result illustrates that the minimum energy for trapped protons can penetrate shielding to reach PMT is about 200 MeV and trapped electrons have no chance to reach the PMTs. After considering incident angle, the number of protons can reach the PMTs is a much lower proportion in the real situation. So the performance degradation of PMTs from exposure to energetic particles directly can be ignored compared with light irradiation.

5.2. Definition of PMT working lifetime

Nevertheless, as a low earth orbit spacecraft, DAMPE will pass through the SAA region and HLRs several times per day, and these repeated passages through the radiation anomaly region at an accumulated long time would shorten the practical life of the tubes. This degradation even damages to the PMTs is mainly from the irradiation of large numbers of scintillation lights since the immediate damage can be eliminated by adopting particular voltage divider circuits and thick radiation shielding material. In order to evaluate this cumulative effect to the PMT, a definition called working lifetime is provided by the produced corporation Hamamatsu, which means that the gain variation of the PMT should be less than 25% via compared with the initial value which is related to the value of anode current. This definition could be used to judge whether PMT is aging or not. Once aging, performance would be decreased sharply and the noise will be obviously. The relationship between aging speed and accumulative lights is complex. Furthermore, accumulative lights is referred to the total number of scintillation lights. The aging speed is generally proportional to the total radiation lights as they are weak. Once the PMT window is exposed to strong light intensity, the aging speed is not proportional any more. An acceleration factor is adopted to describe the accelerated aging behavior of PMT. It means that although the same light irradiation accumulated, the working lifetime would become

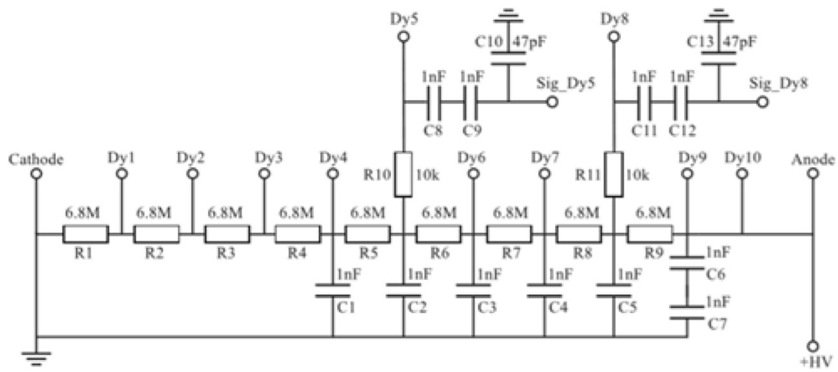

Fig. 11. The circuit of voltage divider adopted by *R*4443.

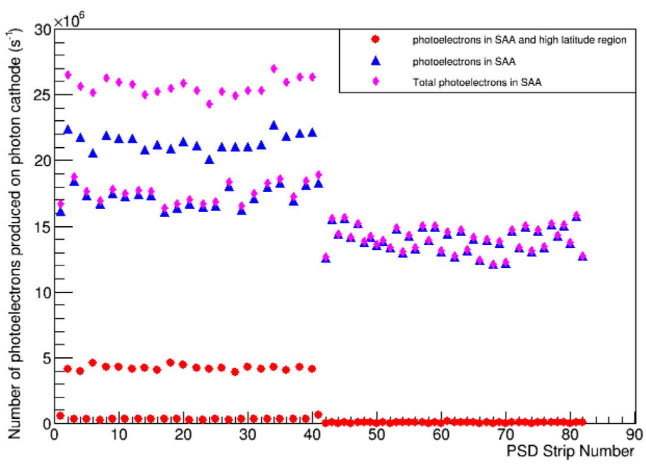

Fig. 12. The distribution of photoelectrons of each PSD strip for the trapped particles. The red circles represent photoelectrons produced per second related to the trapped electron in SAA region and HLRs, and the blue triangles stand for photoelectrons produced per second related to the trapped proton in SAA region. The purple diamond is the total photoelectrons produced per second in SAA region. (For interpretation of the references to color in this figure legend, the reader is referred to the web version of this article.)

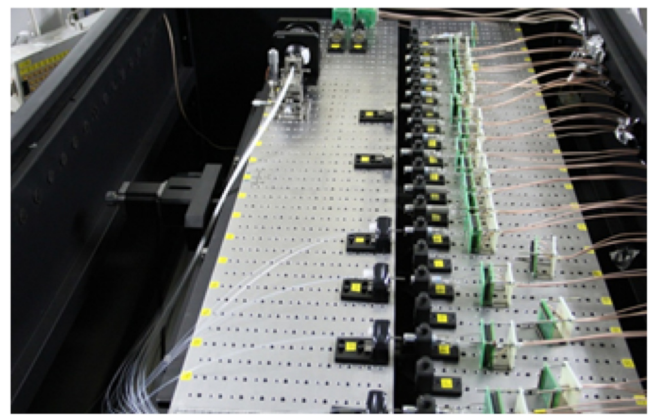

Fig. 13. The test platform for the PMTs.

shorter when the PMT receives massive scintillation photons. In order to describe the lifetime of PMT, a formula is defined as follows:

$$\frac{1}{AF(I^{exp}_{anode})}\cdot\int_0^{T_{exp}} I^{exp}_{anode}dt=\int_0^{T_{Lab}} I^{Lab}_{anode}dt \tag{2}$$

where the right side is the cumulative total anode current within the measured time from a laboratory test, the left side is the cumulative total anode current within the expected time in the orbit. Since the aging speed of PMT is related to the incident light intensity, an accelerated factor (AF) is used to indicate this effect. This factor is a decreasing function of anode current and also refers to a semi-empirical formula provided by the manufacture Hamamatsu Corporation [21]. In general, the signal is extracted by the anode or the last dynodes. But in the PSD, the signals from each PMT are extracted by Dy5 and Dy8 instead of the anode, the expected current and measured current should be revised to the current from Dy8.

5.3. Evaluation of scintillation lights irradiation to the PMTs

As discussed above, the radiation of energetic particles in trap belts haves no damage directly to the PMTs for enough thick shielding material. The damage mainly derives from the scintillation lights, which are produced by TID and converted into photoelectrons via photocathode on PMT window. In the PSD, the signal from Dy8 is the last stage of the readout PMT, so the photoelectrons only multiply eight times in the dynodes system and convert to signal current. A detailed description of an evaluation method of photoelectrons produced by the MIP signal is in Ref. [20]. A MIP signal can produce the average 48 photoelectrons. Also, in the Ref. [20], the gain of Dy8 could be calculated that the value is 6.3×10^4. Once the number of photoelectrons in the inner surface of the PMT window is known, the signal current value from Dy8 can be acquired. The number of photoelectrons produced in the PMT window for each hit could be obtained from the energy deposition of each hit, and then the Dy8 signal current will be calculated. The maximum hit rates of each PSD strip for the trapped particles can be obtained from Fig. 9. To evaluate the maximum total photoelectrons per second, a maximum expected rate of about 540 kHz in orbit as shown in Fig. 9 is adopted to simulate, and the simulation results is shown in Fig. 12. A clear odd–even effect as the same as the hit rates and the TID is also observed for the total number of photoelectrons distribution. The contribution from protons is larger than that from electrons for their different energy deposited behavior in the detection material. Moreover, the PMTs installed at the top layer will suffer the worst scintillation light irradiation environment. Besides, the number of total photoelectrons per second is very different when DAMPE runs in different regions. According to the results given by Fig. 12, the maximum number of photoelectrons from the top layer is 2.7×10^7 PEs/s in SAA region, 5×10^6 PEs/s in HLRs respectively. After excluding the SAA region and HLRs, the redundant normal region is also evaluated by assuming maximum hit rate of 1 KHz which is actually far greater than the actual situation. To DAMPE, the protons with an energy level of MIPs, mostly from the galaxy, contribute to the TIDs of the PSD strips in the normal region, and the number of photoelectrons from the top layer is less than 4.8×10^4 PEs/s in this region. Considering the gain of Dy8, it is deduced that the average Dy8 signal current in the SAA region, HLRs and normal region are 0.272 uA, 0.0504 uA and 0.484 nA respectively.

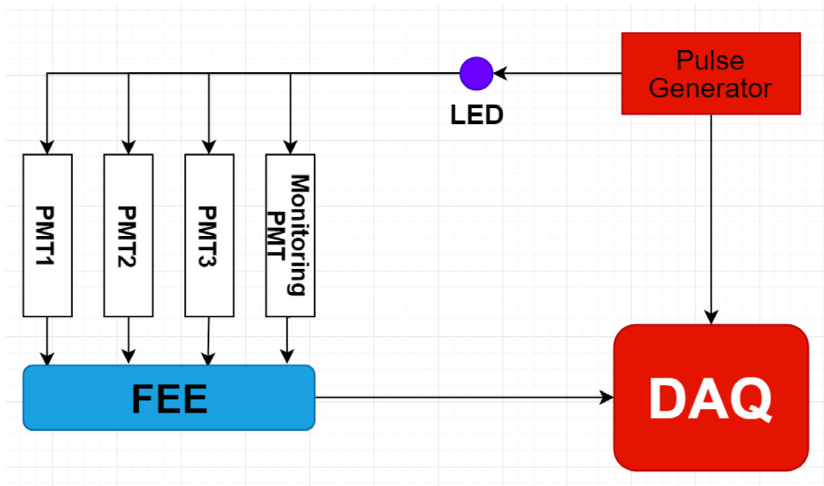

Fig. 14. The layout of the LED test in laboratory.

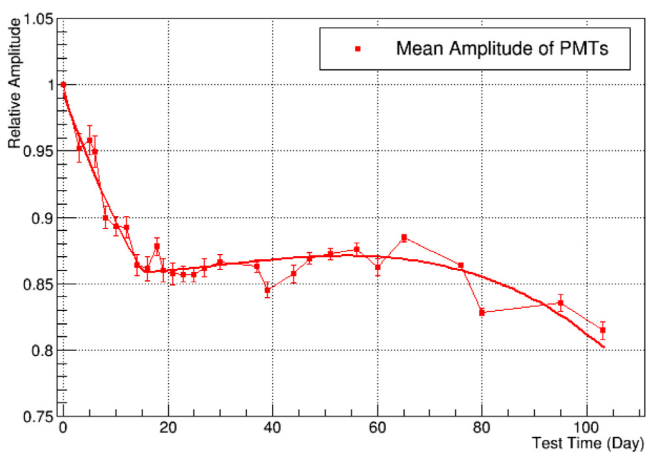

Fig. 15. The relative amplitude of Dy8 for each PMT versus time.

5.4. Evaluation of working lifetime for the PMTs at laboratory

According to the formula (1), the cumulative total anode current within an operating time is important to evaluate the expected working lifetime in orbit. A LED test platform [22] was established, as shown in Fig. 13, to measure the operating time in the laboratory. The layout of the LED platform in the laboratory is shown in Fig. 14. There were four R4443 PMTs with the same version in-flight model used totally. Three of them were used to obtain the laboratory working lifetime, and the remaining one was used as a reference PMT to monitor the light amplitude change of the LED. The measured PMTs were exposed to the LED continuously, while the monitoring PMT only powered on in measuring time. The LED was pulsed by a pulse generator AFG3252 produced by Tektronix Corporation and split into four parts through fibers. The front end electronic (FEE) and the data acquisition system (DAQ) were the same as the flight model of the PSD. For evaluating the performance of the PMTs under in a harsh light radiation environment, the pulse frequency was set to be a very large value 1MHz, and the signal amplitude of the LED from Dy8 was equivalent to the signal amplitude from MIPs as passing through the PSD strips in vertical. A current value of Dy8 was calculated to be 0.484 uA. At this current value, the gain of each PMT decreased by around 20% after 103 days LED irradiation. It is noteworthy that the gain degradation value (20%) is less than the value (25%) provided by Hamamatsu Corporation. Fig. 15 shows the experimental result.

5.5. Evaluation of working lifetime for PSD-PMT

The maximum dynode current in the orbit has been evaluated, meanwhile the working lifetime has been measured at the laboratory, so the expected minimum lifetime of the PMTs in the PSD can be calculated. Furthermore, a detailed equation based on formula 4.1 can be rewritten as follows:

$$\begin{aligned}&\frac{1}{AF(I_{SAA})}\cdot I_{SAA}\cdot 5\%T_{exp}+\frac{1}{AF(I_{HLR})}\cdot I_{HLR}\cdot 30\%T_{exp}\\&+\frac{1}{AF(I_{NR})}\cdot I_{NR}\cdot 65\%T_{exp}=I_{Lab}\cdot T_{Lab}\end{aligned} \tag{3}$$

where I_{Lab} is the dynode current of Dy8 from a laboratory test with LED, and T_{Lab} is the working lifetime in the laboratory as the PMT has 20% gain degradation related to the initial gain, and T_{exp} is the expected working lifetime in the orbit as the initial gain degradation reaches to 20%. The values 5% and 30% are the maximum ratios of the whole operating time of DAMPE in the SAA region and HLRs. $AF(I_{SAA})$, $AF(I_{HLR})$ and $AF(I_{NR})$ are the accelerated factors at three different regions, and the relationships among $AF(I_{SAA})$, $AF(I_{HLR})$ and $AF(I_{NR})$ meet the requirement as follows:

$$\frac{1}{AF(I_{NR})}\ll\frac{1}{AF(I_{HLR})}<\frac{1}{AF(I_{SAA})}<1 \tag{4}$$

After substituting dynode current calculated in different regions as the previous evaluation, the expression of T_{exp} can be calculated as follows:

$$T_{exp}\approx\frac{0.484uA\cdot 103d}{0.0136uA\cdot\frac{1}{AF(I_{SAA})}+0.0151uA\cdot\frac{1}{AF(I_{HLR})}} \tag{5}$$

Due to the maximum possible current in the SAA region is the same order of magnitude as the laboratory LED test, so it is considered that AF in SAA region is approximately equal to 1. Besides, in order to simplify the nonlinear problem of AF, the relationship between AF in the SAA region and HLRs can be regarded to be linear roughly. Based on the above assumptions, the expression of T_{exp} can be simplified further as follows:

$$\begin{aligned}T_{exp}&\approx\frac{0.484uA\cdot 103d}{0.0136uA+0.0151uA\cdot\frac{AF(I_{inSAA})}{AF(I_{inHLR})}}\\&\approx\frac{0.484uA\cdot 103d}{0.0136uA+0.0151uA\cdot\frac{I_{inHLR}}{I_{inSAA}}}=8.32y\end{aligned} \tag{6}$$

The calculated result illustrates that the minimum working lifetime of the PMTs is 8.32 years as the gain of the PMTs at the top layer is degraded by 20%. Due to the simplification of AF, the denominator of formula (6) is larger than the real situation. Moreover, the total

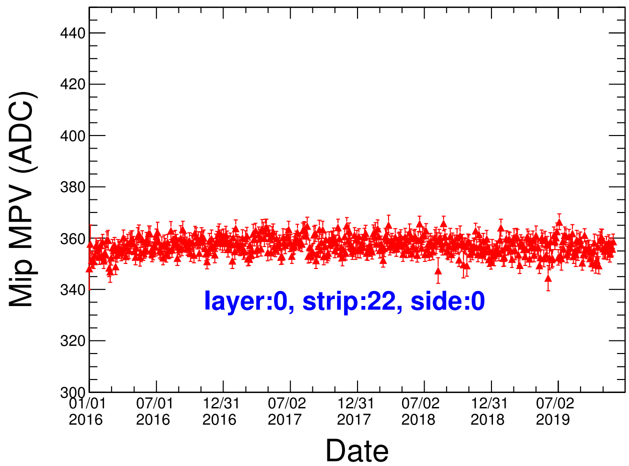

Fig. 16. The most probable value (MPV) of MIP signals versus time.

operation time in the SAA region and HLRs is overestimated compared with the actual situation. These two reasons lead to the underestimation of the real working lifetime, and the expected value of the PMTs of the even strips at the top layer should be longer than 8.32 years.

Now DAMPE has been running for more than four years, and in-orbit calibration results indicate the DAMPE is in good working conditions [23]. During these four years, the high voltage of each PMT has been unchanged, and the temperature for the PSD is stable within 1°. Fig. 16 shows the amplitude of the MIP signal related to the PMT gain changes with time in the orbit. The result illustrates that the PMT is not aging after more than 4 years. It is shown that there is difference in gain variation between Figs. 15 and 16. The reason is that the adopted PMTs in the laboratory and the PMTs in orbit face different light irradiation conditions. The PMTs adopted in the Lab suffered a harsher continuous light irradiation in an aging test. Although the maximum possible current in the SAA region is the same order of the magnitude as the instantaneous intensity of the LED irradiation in the laboratory, the DAMPE satellite passes the SAA region for several minutes in one orbit and always less than the maximum current in this region. That makes an overestimation of the actual TID, and the PMTs also benefit from the intermittent mode of the satellite passing through the SAA region and has a chance to recover from fatigue.

6. Conclusion

As a very high energy astronomical apparatus, evaluation of the working lifetime of DAMPE detection parts is meaningful since it can help the scientific users of DAMPE to evaluate the final statistics of high energy particles. Due to the PSD will meet a worse radiation environment, so it is meaningful to take the PSD to evaluate space radiation damage to DAMPE. Compared with electronics, there are few surveys about the radiation effect of the plastic scintillator detectors readout by PMTs. In order to investigate the space TAD damage to the scintillator strips and the PMTs of the PSD, a detailed evaluation method combining Spenvis and DMPSW are adopted to survey the space radiation of the PSD. A maximum hit rate of about 540 KHz of the top layer strips in the PSD and a dose of 4 Gy per year illustrates that radiation damage to the PSD strips can be completely ignored. Due to enough thick shielding material for the readout PMTs, the radiation damage from direct exposure to the energetic particles is neglected, so the radiation damage source for the PMTs is mainly from scintillation photons. Beyond the Geant4 simulation, a LED test platform is established to obtain the working lifetime of the PMTs at the laboratory with a very high pulsed frequency 1 MHz. Ultimately, the minimum lifetime of the PMTs in the PSD is 8.32 years as the gain of the PMTs installed at the top layer of the PSD is degraded by 20%, which value is less than the manufacture provided. Also, from more than three years of operation in orbit, the gain of each PMT has no degradation. In a word, the detection part of the PSD is not the critical factor to influence the working life of the whole apparatus.

CRediT authorship contribution statement

Yongjie Zhang: Writing - original draft, Formal analysis, Investigation. **Zhiyu Sun:** Writing - review & editing, Conceptualization, Methodology. **Yuhong Yu:** Writing - review & editing, Conceptualization, Methodology, Supervision. **Jianhua Guo:** Resources, Investigation. **Fang Fang:** Investigation, Data curation. **Yong Zhou:** Resources, Software, Investigation. **Zhaoming Wang:** Investigation. **Yapeng Zhang:** Formal analysis, Validation. **Bitao Hu:** Validation.

Declaration of competing interest

The authors declare that they have no known competing financial interests or personal relationships that could have appeared to influence the work reported in this paper.

Acknowledgments

This work was funded by the National Key Research and Development Program of China (2016YFA0400201), and was also supported by the National Natural Science Foundation of China (Grant Nos. U1738129, 11703062, U1738205, U1832122, U1831206, 11622327).

References

[1] Chang Jin, Dark matter particle explorer: The first Chinese cosmic ray and hard $\gamma - ray$ detector in space, Chin. J. Space Sci. 5 (2014) 550–557.
[2] DAMPE Collabration, Direct detection of a break in the teraeletronvolt cosmic-ray spectrum of electrons and positrons, Nature 552 (2017) 63–66.
[3] Qiang Yuan, Lei Feng, Dark matter particle explorer observations of high-energy cosmic ray electrons plus positrons and their physical implications, Sci. China-Phys. Mech. Astron. 61 (2018) 101002.
[4] DAMPE Collabration, Measurement of the cosmic ray proton spectrum from 40 GeV to 100 GeV with the DAMPE sattellite, Sci. Adv. 5 (2019) eaax3793.
[5] E. Fermi, On the origin of the cosmic radiation, Phys. ReV. 75 (1949) 1169–1174.
[6] M. Aguilar, L. Ali Cavasonza, G. Ambrosi, et al., Precision measurement of the boron to carbon flux ratio in cosmic rays from 1.9 GV to 2.6 TV with the alpha magnetic spectrometer on the international space station, Phys. Rev. Lett. 117 (2016) 231102.
[7] E.J. Daly, J. Lemaire, D. Heynderickx, D.J. Rodgers, Problems with models of the radiation belts, IEEE Trans. Nucl. Sci. 43 (1996) 403–415.
[8] J. Chang, G. Ambrosi, Q. An, et al., The dark matter particle explorer mission, Astro. Phys. 95 (2017) 6–24.
[9] Yuhong Yu, Zhiyu Sun, Hong Su, et al., The plastic scintillator detector for DAMPE, Astro. Phys. 94 (2017) 1–10.
[10] Tiekuang Dong, Yapeng Zhang, Pengxiong Ma, et al., Charge measurement of cosmic ray nuclei with the plastic scintillator of DAMPE, Astro. Phys. 105 (2019) 31–36.
[11] P. Azzarello, G. Ambrosi, R. Asfandiyarov, et al., The DAMPE silicontungsten tracker, Nucl. Instrum. Methods Phys. Res. A 831 (2016) 378–384.
[12] Yifeng Wei, Yulong Zhang, Zhiyong Zhang, et al., Performance of the DAMPE BGO calorimeter on the ion beam test, Nucl. Instrum. Methods Phys. Res. A 922 (2019) 177–184.
[13] Eljen technology, http://www.eljentechnology.com/.
[14] Momentive corporation, https://www.momentive.com/.
[15] http://www.spenvis.oma.be/.
[16] Chi Wang, Dong Liu, Yifeng Wei, et al., Offline software for the DAMPE experiment, Chin. Phys. C 10 (2017) 106201.
[17] http://geant4.web.cern.ch.
[18] V. Bindi, D. Casadei, G. Castellini, et al., Performance of AMS-02 time of flight, in: 29th International Cosmic Ray Conference Pune, Vol. 9, 2005, pp. 41–44.
[19] Li Zhao, Wu Chong, Heng Yuekun, et al., Properties of plastic scintillators after irradiation, Nucl. Instrum. Methods Phys. Res. A 552 (2015) 449–455.
[20] Yong Zhou, Zhiyu Sun, Yuhong Yu, et al., A large dynamic range readout design for the plastic scintillator detector of DAMPE, Nucl. Instrum. Methods Phys. Res. A 827 (2016) 79–84.
[21] Hamamatsu corporation, https://www.hamamatsu.com/.
[22] Yong Zhou, Zhiyu Sun, Yuhong Yu, et al., A versatile test bench for photomultiplier tube characterization and it's application in the DAMPE-PSD, Nucl. Sci. Tech. 27 (2016) 70.
[23] G. Ambrosi, Q. An, R. Asfandiyarov, et al., The on-orbit calibration of DArk Matter Particle Explorer, Astro. Phys. 106 (2019) 18–34.